**Climate
of the Past**
Open Access
Discussions

Impact of the oceanic geothermal heat flux on a glacial ocean state

M. Ballarotta[1,2], **F. Roquet**[3,2], **S. Falahat**[4,2], **Q. Zhang**[1,2], and **G. Madec**[5,6]

[1]Department of Physical Geography, Stockholm University, Stockholm, Sweden
[2]Bolin Centre for Climate Research, Stockholm University, Stockholm, Sweden
[3]Department of Meteorology, Stockholm University, Stockholm, Sweden
[4]Department of Environmental Science and Analytical Chemistry, Stockholm University, Stockholm, Sweden
[5]Sorbonne Universités (UPMC, Université Paris 06)-CNRS-IRD-MNHN, LOCEAN Laboratory, Paris, France
[6]National Oceanography Centre, Southampton, Marine Systems Modelling Group, Southampton, UK

Correspondence to: M. Ballarotta (maxime.ballarotta@natgeo.su.se)

Discussion Paper | Discussion Paper | Discussion Paper | Discussion Paper

CPD

11, 3597–3624, 2015

Impact of the oceanic geothermal heat flux on a glacial ocean state

M. Ballarotta et al.

Title Page

Abstract	Introduction
Conclusions	References
Tables	Figures

|◄ | ►|
◄ | ►

Back | Close

Full Screen / Esc

Printer-friendly Version

Interactive Discussion

Abstract

The oceanic geothermal heating (OGH) has a significant impact on the present-day ocean state, but its role during glacial periods, when the ocean circulation and stratification were different from those of today, remains poorly known. In the present study, we

5 analyzed the response of the glacial ocean to OGH, by comparing ocean simulations of the Last Glacial Maximum (LGM, ~ 21 ka ago) including or not geothermal heating. We found that applying the OGH warmed the Antarctic Bottom Waters (AABW) by ~ 0.4 °C and increased the abyssal circulation by 15 to 30 % north of 30° S in the deep Pacific and Atlantic basins. The geothermally heated deep waters were then advected toward

10 the Southern Ocean where they upwelled to the surface due to the Ekman transport. The extra heat transport towards Antarctica acted to reduce the amount of sea ice contributing to the freshening of the whole AABW overturning cell. The global amount of salt being conserved, this bottom freshening induced a salinification of the North Atlantic and North Pacific surface and intermediate waters, contributing to the deepening

15 of the North Atlantic Deep Water. This indirect mechanism is responsible for the largest observed warming, found in the North Atlantic deep western boundary current between 2000 and 3000 m (up to 2 °C). The characteristic time scale of the ocean response to the OGH corresponds to an advective time scale (associated with the overturning of the AABW cell) rather than a diffusive time scale. The OGH might facilitate the transi-

20 tion from a glacial to an inter-glacial state but its effect on the deep stratification seems insufficient to drive alone an abrupt climate change.

1 Introduction

The oceanic geothermal heating (OGH) is the heat flux through the sea floor which is generated by the internal heat content of the lithosphere. This flux is maximum near

25 the oceanic ridges or underwater volcanic regions and is minimum (~ 50 mW m^{-2}) in

Impact of the oceanic geothermal heat flux on a glacial ocean state

M. Ballarotta et al.

the abyssal plains (see e.g. Stein and Stein, 1992; Davies and Davies, 2010; Goutorbe et al., 2011).

The importance of the OGH as a heat source for the ocean system has long been controversial. Although the ocean is largely heated and thermally driven at the surface, several recent studies suggest that the OGH can also affect the ocean dynamic and heat budget (Scott et al., 2001; Adcroft et al., 2001; Emile-Geay and Madec, 2009; Hofmann and Maqueda, 2009; Urakawa and Hasumi, 2009; Hieronymus and Nycander, 2012; Mashayek et al., 2013; de Lavergne et al., 2015). By applying spatially constant or variable heat flux in Ocean General Circulation Models (OGCMs) forced with the present day climate, it is shown that the OGH is a significant forcing that can weaken the stability of the water column, warm the bottom water and strengthen the thermohaline circulation (~ 5 Sv, Sv $= 10^6$ m^3 s^{-1}).

Sparse observations suggest that the high oceanic heat fluxes are important factors causing regional bottom water changes on centennial time scale, such as the observed thermal change in the abyssal subarctic Pacific Ocean (Joyce et al., 1986) and in the deep Eurasian Basin of the Arctic ocean (Björk and Winsor, 2006), or the rapid deep water renewal associated with spreading centres (Detrick et al., 1974; Hautala et al., 2005). A recent study based on laboratory experiment supports the strong effect of the OGH on local scale but minimises its impact on the thermohaline circulation and the turbulent mixing (Zhou et al., 2014).

From a paleo-climate perspective, the abrupt release of potential energy due to the accumulation of OGH in the deep ocean is invoked for explaining the rapid temperature variations observed in reconstructions of the last glacial cycles based on ice and sediment cores (Adkins et al., 2005). It is also postulated that the OGH could have a large impact on the glacial overturning circulation and the deep water properties, such as the deep CO_2 storage. A climate simulation of the Neoproterozoic Era (~ 700 Ma ago), when the Earth was entirely covered by ice (the so-called Snowball Earth), reveals that the ocean is not stagnant and that the OGH may be a driver of its dynamic in decreasing the density of the abyssal waters, enhancing the convective vertical mixing and

homogeneous temperature and salinity in the water column (Ashkenazy et al., 2013, 2014).

To our knowledge, the impact of the OGH has not been yet investigated for more recent glacial climate period, such as the Last Glacial Maximum (LGM, ~ 21 ka ago), when the conditions were colder, the atmospheric CO_2 concentration was lower (Monnin et al., 2001) and the ocean stratification and deep circulation stronger than those found today (see e.g., Duplessy et al., 1988; Sarnthein et al., 1994; Adkins et al., 2002; Adkins and Schrag, 2003; Curry, 2005; Lynch-Stieglitz et al., 2007; Otto-Bliesner et al., 2007). In the present study, we explored the impact of the OGH on a glacial ocean state by using the forced LGM configuration of Ballarotta et al. (2013a). We aimed at (1) evaluating the impact of the OGH on the ocean circulation, in particular the North Atlantic and abyssal thermohaline circulation, the advective heat transport and the stratification; and (2) testing whether the OGH could be a trigger of transition between glacial and interglacial climate. The paper is organised as follows: the ocean simulations are described in Sect. 2; the impact of the OGH on the LGM simulated state is described in Sect. 3; Results are discussed in Sect. 4 and a conclusion is given in Sect. 5.

2   Model description

The NEMO-LIM2 model (Madec, 2008) was used to design the numerical experiments. The model configuration was similar to the experiment made by Emile-Geay and Madec (2009) in their study on the impact of the OGH in the present-day climate. NEMO solves the primitive equations discretised on a curvilinear horizontal mesh and was based in our study on a 2° × 2° Mercator grid (namely the ORCA2 global configuration). Within the tropics, the meridional resolution is increased up to 0.5°. The vertical dimension is discretised into 31 unevenly spaced depth levels (10 m at the surface and 500 m in the deep ocean). The LGM bathymetry is derived from the present-day bathymetry minus 120 m, representative of the alteration of the sea level due to the freshwater storage in the continental ice-sheets during the LGM. The vertical eddy viscosity and

diffusivity coefficients required to model the vertical mixing were computed from the Turbulent Kinetic Energy (TKE) turbulent closure model (Gaspar et al., 1990; Blanke and Delecluse, 1993; Madec, 2008). The NEMO model uses the TEOS-10 equation of state (Roquet et al., 2015). The parameterisation of the mesoscale eddy-induced turbulence was established by the Gent and McWilliams (1990) formulation, which associates an eddy-induced velocity to the isoneutral diffusion. The ocean is coupled to the Louvain-La-Neuve Ice Model LIM2 (Fichefet and Maqueda, 1997; Timmermann et al., 2005) which solves the thermodynamic growth and decay of the sea ice, the sea ice dynamic and its transport.

NEMO-LIM2 was initialised at rest and with the temperature, salinity and sea-ice fields averaged over the last 100 years of a 4000 years long LGM experiment carried out with the MPI-OM coupled model (Zhang et al., 2013). The surface boundary conditions are computed using the CORE bulk formulae (Large and Yeager, 2004) and the atmospheric fields from a LGM quasi-equilibrated climate model experiment (Brandefelt and Otto-Bliesner, 2009). Note that no restoring sea surface salinity term was applied but the freshwater budget was constrained to have an instantaneous zero global mean value. A more exhaustive presentation of the experimental setup and boundary conditions can be found in Ballarotta et al. (2013a).

For the present study, we designed a reference experiment (REF) without OGH at the sea floor. In a second experiment (GH), spatially varying OGH fluxes were applied as the bottom boundary condition. Following Emile-Geay and Madec (2009), the OGH is computed from the age of the bedrock. We assumed that the OGH flux during the LGM was the same as today, since it is estimated from the age of the bedrocks expressed in million of years and that the LGM continental plate arrangement was similar to the modern day condition. The total energy input from the OGH forcing is 29.9 TW (TW = 10^{12} W) and the mean value over the ocean is $\sim 88\,\mathrm{mW\,m^{-2}}$. This OGH forcing modifies the heat content by changing the temperature trend in the model grid boxes just above the ocean floor.

Full Screen / Esc

For each configuration, NEMO was integrated for $\sim 14\,000$ years and the analysis covered the last 100 model-years. At this stage of the integration, the ocean model was close to equilibrium. The annual mean model drifts both in temperature and salinity was weak, with $< 0.006\,°C\,\text{century}^{-1}$ ($< 0.003\,°C\,\text{century}^{-1}$) below 500 m and $< 0.09\,°C\,\text{century}^{-1}$ ($< 0.08\,°C\,\text{century}^{-1}$) in the upper 500 m for REF (GH). The model drift in salinity was also weak for both GH and REF, with $< 0.004\,\text{PSU century}^{-1}$ below 500 m and $< 0.012\,\text{PSU century}^{-1}$ in the upper layer.

3 Results

3.1 Impact of the geothermal heat flux on the stratification

The annual mean temperature drift induced by the OGH as a function of depth is shown in Fig. 1a, b averaged over the Atlantic and the Indo-Pacific basins, respectively. In the GH experiment, the Atlantic basin is $\sim 0.4\,°C$ colder above 1500 m and gains heat below 1500 m with a maximum warming of $\sim 0.9\,°C$ formed between 2000 and 3000 m. In the Indo-Pacific basin, the upper 1500 m layer is $\sim 0.25\,°C$ warmer, whereas the deep layer is up to $0.4\,°C$ warmer. In the Atlantic basin, the heat accumulation due to the OGH below 1500 m has a characteristic time scale of ~ 1600 years and reaches an asymptotic limit of $0.38\,°C$ (Fig. 1c). In the Indo-Pacific basin, the characteristic time scale is ~ 1200 years and the accumulated heat reaches an asymptotic limit of $0.31\,°C$. An equilibrium is reached after $\sim 10\,000$ years.

The annual zonal mean temperature and salinity patterns in REF for the Atlantic and the Indo-Pacific basins are shown in Fig. 2a–d. The deep ocean is filled with cold (near the freezing point of sea-water) and saline waters, which agrees with paleo-proxy reconstructions (Adkins et al., 2002; Adkins and Schrag, 2003) and the simulation by Brandefelt and Otto-Bliesner (2009). Relatively fresh and cold waters are found between 40 and 90° N in the North Atlantic and North Pacific basins, due to the presence of sea ice.

Impact of the oceanic geothermal heat flux on a glacial ocean state

M. Ballarotta et al.

Title Page

Abstract	Introduction
Conclusions	References
Tables	Figures

◀	▶	
◀	▶
Back	Close

Full Screen / Esc

Printer-friendly Version

Interactive Discussion

The impact of the OGH on the zonal mean temperature and salinity patterns is shown in Fig. 2e–h. The temperature differences are significant at all depth except in the upper 200 m where the temperature variability is strong and mainly controlled by the atmospheric state. The North Atlantic cooling found in Fig. 1 is mainly associated with colder surface water in the Nordic Seas (up to 0.7 °C colder) and with the intrusion of colder Antarctic Intermediate Water (AAIW) in the South Atlantic basin (up to 1.3 °C colder). The deep temperatures in the Atlantic Ocean are up to 1.3 °C warmer, particularly between 1500 and 3000 m in the deep western boundary current (Fig. 3), and between 30 and 45° N. In the Indo-Pacific basin, the layer below 1500 m is up to 0.4 °C warmer and the surface layer is slightly colder (0.1 °C colder) in the North Pacific basin and ∼ 0.3 °C warmer in the South Pacific. The salinity differences are significant at all depth and the patterns are relatively similar between the Atlantic and the Indo-Pacific basins: the Antarctic Bottom Water (AABW) is ∼ 0.1 PSU fresher in GH than in REF whereas the upper layer is between 0.1 and 0.3 PSU saltier.

These differences in the temperature and salinity patterns modify the sea-water density (Fig. 4). The AABW becomes less dense (the density decreases by ∼ 0.2 kg m^{-3} in the Indo-Pacific, 0.3 kg m^{-3} in the Atlantic) due to warming and freshening, whereas the density increases up to 0.3 kg m^{-3} in the thermocline due to colder and more saline waters. The stratification is hence increased by ∼ 3 % near 2250 m and is reduced by ∼ 3 % near 3250 m (not shown).

3.2 Impact of the geothermal heat flux on the thermohaline circulation

Most paleo-climate studies investigate the thermohaline circulation in the latitude-depth coordinates. A better description of the circulation is however found in latitude-density coordinates (Döös, 1994; Döös and Webb, 1994; Ballarotta et al., 2013b). Ballarotta et al. (2014) have also shown that the strength of the glacial overturning strongly depends on the choice of coordinate system. Therefore, we present hereafter the meridional overturning circulation (MOC) in latitude-density coordinates, more precisely σ_4 (i.e., referenced to 4000 m), in order to better capture and compare the abyssal circu-

Impact of the oceanic geothermal heat flux on a glacial ocean state

M. Ballarotta et al.

Back | Close

Full Screen / Esc

Printer-friendly Version

Interactive Discussion

lation. Because the OGH affects the ocean's density structure, subtracting the stream-functions latitude-density coordinates is meaningless. It is however possible to identify the maximum of the AABW transport at each latitude, as well as the density where the waters are formed. The MOC in latitude-depth coordinates is presented and discussed in the Appendix for the reader who is not familiar with the MOC in latitude-density coordinates.

The annual mean effective (Eulerian mean + eddy induced velocities) MOC in latitude-density coordinates is shown in Fig. 5, for REF and GH. In the Southern Ocean, relatively dense waters ($\sigma_4 > 46.2\,\mathrm{kg\,m^{-3}}$) are formed between 60 and 80° S. These waters are then transported almost adiabatically up to 40° N. The OGH intensifies the AABW cell by 15–30 % (from 20.5 Sv in REF to 23.4 Sv in GH in the Southern Ocean, 3.0 to 3.7 Sv in the Atlantic basin, 6.3 to 8.4 Sv in the Indo-Pacific basin) and shifts the maximum overturning towards lighter density classes (from $\sigma_4 \sim 47.8\,\mathrm{kg\,m^{-3}}$ to $\sigma_4 \sim 47.6\,\mathrm{kg\,m^{-3}}$). The transport associated with the North Atlantic Deep Water (NADW) is ~ 4 Sv stronger in GH than in REF along the 46.5–46.7 kg m^{-3} isopycnals and the maximum of the North Atlantic overturning is 11 % larger in GH (17.2 Sv) than in REF (15.4 Sv). The MOC in latitude-density coordinates also shows the denser NADW in GH than in REF. Associated with it, the volume of the AABW in the Atlantic basin is eroded by ~ 15 % in GH than in REF after 6000 model years (Fig. 6) when the layer below 1500 m is warmed by $\sim 0.3\,^{\circ}$C. In the Indo-Pacific basin, the volume of the AABW is slightly larger (0.3 %).

3.3 Impact on the northward heat transport

The annual mean effective (computed from Eulerian mean + eddy induced velocities) northward heat transport (in PW $= 10^{15}$ W) for the Global Ocean, the Atlantic basin and the Indo-Pacific basin in REF is shown in Fig. 7. In the Indo-Pacific basin, the heat transport reaches maxima of 1 and 2 PW at 14° N and 14° S, respectively, and is directed northward in the Northern Hemisphere, southward in the Southern Hemi-

Title Page

Abstract | Introduction

Conclusions | References

Tables | Figures

|◄ | ►|

◄ | ►

Back | Close

Full Screen / Esc

Printer-friendly Version

Interactive Discussion

Full Screen / Esc

Printer-friendly Version

Interactive Discussion

sphere. In the Atlantic basin, the heat transport is directed towards the North pole at all latitude and is maximum near 22° N (~ 0.9 PW). In the Southern ocean, the heat transport is less than 0.5 PW and directed towards Antarctica. The impact of the OGH on the northward heat transport is statistically significant (based on a *t* test, *p* value less than 5 %) in the Atlantic and Southern oceans. The AABW in the Indo-Pacific basin gains geothermal heat when it spreads northward. Most of this heat (~ 0.03 PW) is exported to the Southern Ocean surface where it diverges towards Antarctica (~ 0.02 PW) and towards the South Atlantic Ocean (~ 0.05 PW) near 50° S. The geothermal heat transported towards Antarctica then participates in the relative freshening of the Southern Ocean surface water. The geothermal heat in the South Atlantic is transported northward and reaches a maximum of ~ 0.12 PW near 40° N, where the maximum mixed layer depths are found.

3.4 Impact on the North Atlantic deep convection

Our results suggest that the impact of the OGH on the glacial ocean stratification and thermohaline circulation is significant. The OGH warms the AABW by ~ 0.4 °C and increases the abyssal circulation between 15 and 30 % north of 30° S in the deep Pacific and Atlantic basins. The geothermally heated deep waters are advected by the deep overturning cell and upwell at the Southern Ocean surface. When reaching the Southern Ocean surface, these waters diverge near 50° S towards Antarctica and towards the North Atlantic basin, due to the Ekman transport. The transport towards Antarctica contributes to the freshening of the surface waters. As a result, the newly formed AABW becomes less saline. Due to the global salt conservation, the freshening of the AABW is compensated by more saline surface waters in the North Atlantic and North Pacific (~ 0.2 PSU saltier), favouring the densification and the deepening of the NADW. The largest warming is hence found in the North Atlantic deep western boundary current between 2000 and 3000 m due to the deepening of the thermocline. Consequently, the volume of AABW is reduced by 15 % in the Atlantic basin. We found that this mechanism is relatively fast and has a characteristic time scale of ~ 1500 years. It corre-

sponds mainly to an advective time scale (associated with the dynamic of the AABW) rather than a diffusive time scale.

4   Discussion

The $\sim 0.4\,^{\circ}$C warming of the abyssal ocean due to OGH is similar to the results found in simulation of the present-day climate (Adcroft et al., 2001; Emile-Geay and Madec, 2009; Hofmann and Maqueda, 2009). However, the largest temperature difference is found between 1500 and 3000 m in the Atlantic basin due to the deepening of the thermocline. This latest result coincides with the result found by Hofmann and Maqueda (2009) in their present-day climate simulations where the North Atlantic deep western boundary current warms between 0.9 and 1.5 $^{\circ}$C, but it contrasts from the solution found in the simulations from Adcroft et al. (2001) and Emile-Geay and Madec (2009) where the largest warming takes place in North Pacific below 3000 m depth. The mechanism, explained above, is compatible with the results found in Hofmann and Maqueda (2009). Both in our study and in Hofmann and Maqueda (2009), and in opposition to Emile-Geay and Madec (2009) and other studies, the ocean surface salinity is not relaxed towards a climatology. Therefore, the warming of the abyssal waters contributes to freshening of the Southern Ocean surface waters via the advection of heat. The large formation of AABW contributes to fresher (reduced salinity) abyssal waters. Due to the closed freshwater budget and no restoring term in the sea surface salinity in the model, the Southern Ocean freshwater supply is counter-balanced by the densification of the surface waters becoming more saline in the North Atlantic and Pacific Ocean. As a result, the AMOC is reinvigorated by the increased surface salinity.

We found that the maximum of the AMOC is ~ 11–15 % larger in GH than in REF, which is similar to the value found in simulation of the the present-day climate (Hofmann and Maqueda, 2009). This value may be considered as relatively important in light of the estimation made for the future climate scenarios (an average reduction of 25 % in Meehl et al. (2007) or on short time scale, but it is relatively weak compared

to the variation of the AMOC on climate time scale, such as the 75 % reduction with respect to LGM period during Heinrich stadial 1 (∼ 15–18.5 ka ago), the 45 % reduction during the Younger Dryas stadial (∼ 12 ka ago) (Ritz et al., 2013), or the values found in fresh water hosing experiments under LGM conditions (> 20 % reduction in Kageyama et al., 2013). In these experiments, the AMOC changes are linked with surface processes, such as the freshwater discharge (Heinrich, 1988; Hemming, 2004) which have a stronger and faster impact on the thermohaline circulation than the processes induced by the OGH.

Similar to Adcroft et al. (2001) and Emile-Geay and Madec (2009), we found that the impact of the OGH on the northward heat transport is weak (∼ 10 %) but non-negligible, particularly in the Atlantic Ocean and in the polar regions as a result of the large scale advection of the abyssal heat content. We found that the alteration of the ocean heat transport induced by the OGH in the North Atlantic (∼ 0.1 PW) is ∼ 3 time larger than the total energy input provided by OGH (0.03 PW). It seems that the Southern Ocean Ekman transport prevents the accumulation of OGH in the abyssal ocean. For a salinity gradient of ∼ 1 PSU, a temperature gradient of ∼ 3 °C would be required to destabilise the water column (see Appendix B). In the present study, the OGH warms by ∼ 0.4 °C. Therefore the OGH alone is not sufficient to destabilise the water column. It seems that OGH facilitates the transition from a glacial to an inter-glacial state by reducing the volume of saline abyssal waters by ∼ 15 % and reinvigorating the North Atlantic overturning by ∼ 10 %, but it is unlikely that the OGH is the only cause to abrupt climate changes.

5   Conclusions

In the present study, we investigated the response of the ocean to the geothermal heat flux during a glacial period, such as the LGM, when the ocean circulation and stratification were different from today. We found that the heat flux at the sea floor is a significant forcing of the deep ocean and the global thermohaline circulation. The

Antarctic Bottom Water participates in the transport of geothermally heated waters from the Indo-Pacific to the North Atlantic basin, indirectly favouring the deep convection in the North Atlantic and contributing to the deepening of North Atlantic Deep Water.

The deep ocean circulation and the OGH hence may speed up the transition from glacial to inter-glacial ocean state by reducing the volume of saline abyssal waters and reinvigorating the North Atlantic overturning. However, a new steady-state is achieved only a few thousands year after OGH is applied wherein the deep stratification, albeit weakened, remains extremely stable due to the strong salinity gradient. We thus find it unlikely that abrupt climate changes could be triggered by the action of OGH alone during the LGM period. However, the OGH should contribute significantly in the transition between glacial and inter-glacial ocean states. The OGH has a strong effect on the ventilation of the abyssal ocean and might modulate the time scale of the overturning, and in turn, the rate of CO_2 release from the deep ocean to the atmosphere.

Our results rely on forced (i.e. prescribed atmospheric conditions) ocean simulation of the LGM period. It thus does not account for possible ocean feedbacks on the atmosphere. Sensitivity study with fully coupled ocean-atmosphere-biochemistry simulations would be useful to assess the impact of the OGH on the global climate system.

Appendix A: Impact of the geothermal heat flux on the thermohaline circulation in latitude-depth coordinates

A In this section, we present the annual mean effective (Eulerian mean + eddy induced velocities) meridional overturning circulation (MOC) in latitude-depth coordinates (Fig. 8a, b). The structure of the LGM thermohaline circulation agrees with the recents findings derived from multiple paleo-proxies (Curry, 2005; Marchitto and Broecker, 2006; Lynch-Stieglitz et al., 2007; Evans and Hall, 2008; Tagliabue et al., 2009; Gherardi et al., 2009; Lippold et al., 2012; Adkins, 2013). The circulation representative of the North Atlantic Deep Water (NADW) in the upper 2000 m has a maximum transport of ~ 17 Sv at 900 m depth near $35°$ N. It is slightly stronger and shal-

lower than in present-day simulations with same NEMO-ORCA2 model (Emile-Geay and Madec, 2009; Lecointre, 2009; Brodeau et al., 2010), due to a larger intrusion of the AABW in the Atlantic basin.

The difference in the MOC between GH and REF is shown in Fig. 8c, d for the Atlantic and Indo-Pacific basins. The impact of the OGH on the thermohaline circulation is statistically significant (based on a t test, p value less than 5 %) in the Atlantic basin, in the Southern Ocean, in the Arctic basin below 1000 m and in the Indo-Pacific basin below 3000 m. The volume transport in the downwelling branch and the deep current of the NADW is up to 5.6 Sv larger. It is mainly associated with the deepening of the NADW in the GH experiment. The maximum of the AMOC is $\sim$ 15 % larger in GH (20 Sv) than in REF (17 Sv). In the Southern Ocean, the volume transport is $\sim$ 4 Sv larger in upwelling branch of the Deacon Cell, between 34 and 60° S. Note that the Deacon Cell is fictitious and mainly appears in latitude-depth coordinates. The Southern Ocean overturning circulation is better described in latitude-density coordinates than in latitude-depth coordinates (Döös, 1994; Döös and Webb, 1994; Ballarotta et al., 2013b), because it removes the fictitious Deacon Cell. The volume transport is $\sim$ 4.1 Sv larger in the deep AABW cell between 45 and 25° S and near Antarctica. In the North Atlantic and North Pacific, the volume transport in the AABW is between 1 and 2 Sv larger.

Appendix B: Ratio between the thermal expansion coefficient (α) and the saline contraction coefficient (β)

The ratio between the thermal expansion coefficient (α) and the saline contraction coefficient (β) is $< \frac{1}{3}$ PSU°C^{-1} in our simulation. It corresponds to the compensation of the variation of potential temperature due to changes of salinity (McDougall, 1987). Hence, for a salinity gradient of $\sim$ 1 PSU, a temperature gradient of minimum $\sim$ 3 °C would be required to destabilise the water column by mixing processes. In the present study, we found that the OGH warms the deep ocean by only 0.4 °C. Therefore the OGH alone is not sufficient to abruptly destabilise the water column.

References

Adcroft, A., Scott, J. R., and Marotzke, J.: Impact of geothermal heating on the global ocean circulation, Geophys. Res. Lett., 28, 1735–1738, doi:10.1029/2000GL012182, 2001. 3599, 3606, 3607

Adkins, J. F.: The role of deep ocean circulation in setting glacial climates, Paleoceanography, 28, 539–561, doi:10.1002/palo.20046, 2013. 3608

Adkins, J. F. and Schrag, D. P.: Reconstructing Last Glacial Maximum bottom water salinities from deep-sea sediment pore fluid profiles, Earth Planet. Sc. Lett., 216, 109–123, doi:10.1016/S0012-821X(03)00502-8, 2003. 3600, 3602

Adkins, J. F., McIntyre, K., and Schrag, D. P.: The salinity, temperature, and δ_{18}O of the glacial deep ocean, Science, 298, 1769–1773, doi:10.1126/science.1076252, 2002. 3600, 3602

Adkins, J. F., Ingersoll, A., and Pasquero, C.: Rapid climate change and conditional instability of the glacial deep ocean from the thermobaric effect and geothermal heating, Quaternary Sci. Rev., 24, 581–594, doi:10.1016/j.quascirev.2004.11.005, 2005. 3599

Ahn, J. and Brook, E. J.: Atmospheric CO_2 and climate on millennial time scales during the last glacial period, Science, 322, 83–85, doi:10.1126/science.1160832, 2008.

Anderson, R. F., Ali, S., Bradtmiller, L. I., Nielsen, S. H. H., Fleisher, M. Q., Anderson, B. E., and Burckle, L. H.: Wind-driven upwelling in the Southern Ocean and the deglacial rise in atmospheric CO_2, Science, 323, 1443–1448, doi:10.1126/science.1167441, 2009.

Ashkenazy, Y., Gildor, H., Losch, M., Macdonald, F. A., Schrag, D. P., and Tziperman, E.: Dynamics of a snowball Earth ocean, Nature, 495, 90–93, doi:10.1038/nature11894, 2013. 3600

Ashkenazy, Y., Gildor, H., Losch, M., and Tziperman, E.: Ocean circulation under globally glaciated snowball Earth conditions: steady-state solutions, J. Phys. Oceanogr., 44, 24–43, doi:10.1175/JPO-D-13-086.1, 2014. 3600

Ballarotta, M., Brodeau, L., Brandefelt, J., Lundberg, P., and Döös, K.: Last Glacial Maximum world ocean simulations at eddy-permitting and coarse resolutions: do eddies contribute to a better consistency between models and palaeoproxies?, Clim. Past, 9, 2669–2686, doi:10.5194/cp-9-2669-2013, 2013a. 3600, 3601

5 Ballarotta, M., Drijfhout, S., Kuhlbrodt, T., and Döös, K.: The residual circulation of the Southern Ocean: which spatio-temporal scales are needed?, Ocean Model., 64, 46–55, doi:10.1016/j.ocemod.2013.01.005, 2013b. 3603, 3609

Ballarotta, M., Falahat, S., Brodeau, L., and Döös, K.: On the glacial and interglacial thermohaline circulation and the associated transports of heat and freshwater, Ocean Sci., 10, 907–921, doi:10.5194/os-10-907-2014, 2014. 3603

10 Björk, G. and Winsor, P.: The deep waters of the Eurasian Basin, Arctic Ocean: geothermal heat flow, mixing and renewal, Deep-Sea Res. Pt. I, 53, 1253–1271, doi:10.1016/j.dsr.2006.05.006, 2006. 3599

Blanke, B. and Delecluse, P.: Low frequency variability of the tropical atlantic ocean simulated by a general circulation model with mixed layer physics, J. Phys. Oceanogr., 23, 1363–1388, 1993. 3601

15 Brandefelt, J. and Otto-Bliesner, B. L.: Equilibration and variability in a Last Glacial Maximum climate simulation with CCSM3, Geophys. Res. Lett., 36, 1–5, doi:10.1029/2009GL040364, 2009. 3601, 3602

Brodeau, L., Barnier, B., Treguier, A.-M., Penduff, T., and Gulev, S.: An ERA40-based atmospheric forcing for global ocean circulation models, Ocean Model., 31, 88–104, doi:10.1016/j.ocemod.2009.10.005, 2010. 3609

20 Curry, W. B.: Glacial water mass geometry and the distribution of δ^{13}C of ΣCO_2 in the western Atlantic Ocean, Paleoceanography, 20, 1–13, doi:10.1029/2004PA001021, 2005. 3600, 3608

Davies, J. H. and Davies, D. R.: Earth's surface heat flux, Solid Earth, 1, 5–24, doi:10.5194/se-1-5-2010, 2010. 3599

25 de Lavergne, C., Madec, G., Le Sommer, J., George Nurser, A. J., and Naveira Garabato, A. C.: On the consumption of Antarctic Bottom Water in the abyssal ocean, J. Phys. Oceanogr., in revision, 2015. 3599

Detrick, R., Williams, D., Mudie, J., and Sclater, J.: The Galapagos spreading centre: bottom-water temperatures and the significance of geothermal heating, Geophys. J. Int., 38, 627–637, doi:10.1111/j.1365-246X.1974.tb05433.x, 1974. 3599

Title Page

Abstract | Introduction

Conclusions | References

Tables | Figures

|◀ | ▶|

◀ | ▶

Back | Close

Full Screen / Esc

Printer-friendly Version

Interactive Discussion

Döös, K.: Semianalytical simulation of the meridional cells in the Southern Ocean, J. Phys. Oceanogr., 24, 1281–1293, 1994. 3603, 3609

Döös, K. and Webb, D.: The deacon cell and the other meridional cells of the Southern Ocean, J. Phys. Oceanogr., 24, 429–442, 1994. 3603, 3609

5 Duplessy, J. C., Shackleton, N. J., Fairbanks, R. G., Labeyrie, L., Oppo, D., and Kallel, N.: Deepwater source variations during the last climatic cycle and their impact on the global deepwater circulation, Paleoceanography, 3, 343–360, 1988. 3600

Emile-Geay, J. and Madec, G.: Geothermal heating, diapycnal mixing and the abyssal circulation, Ocean Sci., 5, 203–217, doi:10.5194/os-5-203-2009, 2009. 3599, 3600, 3601, 3606,
10 3607, 3609

Evans, H. K. and Hall, I. R.: Deepwater circulation on Blake Outer Ridge (western North Atlantic) during the Holocene, Younger Dryas, and Last Glacial Maximum, Geochem. Geophy. Geosy., 9, Q03023, doi:10.1029/2007GC001771, 2008. 3608

Ferrari, R., Jansen, M., Adkins, J., Burke, A., Stewart, A., and Thompson, A.: Antarctic sea ice
15 control on ocean circulation in present and glacial climates, P. Natl. Acad. Sci. USA, 111, 8753–8758, doi:10.1073/pnas.1323922111, 2014.

Fichefet, T. and Maqueda, M. A. M.: Sensitivity of a global sea ice model to the treatment of ice thermodynamics and dynamics, J. Geophys. Res., 102, 12609–12646, doi:10.1029/97JC00480, 1997. 3601

20 Gaspar, P., Grégoris, Y., and Lefevre, J.-M.: A simple eddy kinetic energy model for simulations of the oceanic vertical mixing: Tests at station papa and long-term upper ocean study site, J. Geophys. Res., 95, 16179–16193, doi:10.1029/JC095iC09p16179, 1990. 3601

Gent, P. and McWilliams, J.: Isopycnal mixing in Ocean Circulation models, J. Phys. Oceanogr., 20, 150–155, doi:10.1175/1520-0485(1990)020<0150:IMIOCM>2.0.CO;2, 1990. 3601

25 Gherardi, J. M., Labeyrie, L., Nave, S., Francois, R., Mc-Manus, J. F., and Cortijo, E.,: Glacial-interglacial circulation changes inferred from 231 Pa/230 Th sedimentary record in the North Atlantic region, Paleoceanography, 24, 1–14, doi:10.1029/2008PA001696, 2009. 3608

Goutorbe, B., Poort, J., Lucazeau, F., and Raillard, S.: Global heat flow trends resolved from multiple geological and geophysical proxies, Geophys. J. Int., 187, 1405–1419,
30 doi:10.1111/j.1365-246X.2011.05228.x, 2011. 3599

Hautala, S. L., Johnson, H. P., and Bjorklund, T.: Geothermal heating and the properties of bottom water in Cascadia Basin, Geophys. Res. Lett., 32, L06608, doi:10.1029/2004GL022342, 2005. 3599

Title Page

Abstract | Introduction

Conclusions | References

Tables | Figures

◄ | ►

◄ | ►

Back | Close

Full Screen / Esc

Printer-friendly Version

Interactive Discussion

Heinrich, H.: Origin and consequences of cyclic ice rafting in the northeast Atlantic Ocean during the past 130,000 years, Quaternary Res., 29, 142–152, doi:10.1016/0033-5894(88)90057-9, 1988. 3607

Hemming, S. R.: Heinrich events: massive late Pleistocene detritus layers of the North Atlantic and their global climate imprint, Rev. Geophys., 42, RG1005, doi:10.1029/2003RG000128, 2004. 3607

Hieronymus, M. and Nycander, J.: The budgets of heat and salinity in NEMO, Ocean Model., 67, 28–38, doi:10.1016/j.ocemod.2013.03.006, 2012. 3599

Hofmann, M. and Maqueda, M.: Geothermal heat flux and its influence on the oceanic abyssal circulation and radiocarbon distribution, Geophys. Res. Lett., 36, L03603, doi:10.1029/2008GL036078, 2009. 3599, 3606

Joyce, T. M., Warren, B. A., and Talley, L. D.: The geothermal heating of the abyssal subarctic Pacific Ocean, Deep-Sea Res., 33, 1003–1015, doi:10.1016/0198-0149(86)90026-9, 1986. 3599

Kageyama, M., Merkel, U., Otto-Bliesner, B., Prange, M., Abe-Ouchi, A., Lohmann, G., Ohgaito, R., Roche, D. M., Singarayer, J., Swingedouw, D., and X Zhang: Climatic impacts of fresh water hosing under Last Glacial Maximum conditions: a multi-model study, Clim. Past, 9, 935–953, doi:10.5194/cp-9-935-2013, 2013. 3607

Large, W. G. and Yeager, S. S.: Diurnal to decadal global forcing for ocean and sea-ice models: the data sets and flux climatologies. NCAR Technical Note, NCAR/TN-460+STR, Boulder, Colorado, CGD Division of the National Center for Atmospheric Research, 2004. 3601

Lecointre, A.: Variabilité interannuelle à décénale en atlantique nord et mers nordiques: etudes conjointe d?observations, simulations numériques et réanalyses, PhD thesis, Université Joseph Fourier, Grenoble 1, 2009. 3609

Lippold, J., Luo, Y., Francois, R., Allen, S. E., Gherardi, J., Pichat, S., Hickey, B., and Schulz, H.: Strength and geometry of the glacial Atlantic Meridional Overturning Circulation, Nat. Geosci., 5, 813–816, doi:10.1038/ngeo1608, 2012. 3608

Lynch-Stieglitz, J., Adkins, J. F., Curry, W. B., Dokken, T., Hall, I., Herguera, J. C., Hirschi, J., Ivanova, E., Kissel, C., Marchal, O., Marchitto, T. M., McCave, I. N., Mc-Manus, J. F., Mulitza, S., Ninnemann, U., Peeters, F., Yu, E. F., and Zahn, R.: Atlantic meridional overturning circulation during the Last Glacial Maximum, Science, 316, 66–69, doi:10.1126/science.1137127, 2007. 3600, 3608

Title Page

Abstract | Introduction

Conclusions | References

Tables | Figures

◄ | ►

◄ | ►

Back | Close

Full Screen / Esc

Printer-friendly Version

Interactive Discussion

Madec, G.: NEMO ocean engine, Note du Pôle de modélisation de l'Institut Pierre-Simon Laplace No. 27, Institut Pierre-Simon Laplace, Paris, France, 2008. 3600, 3601

Marchitto, T. M. and Broecker, W. S.: Deep water mass geometry in the glacial Atlantic Ocean: a review of constraints from the paleonutrient proxy Cd/Ca, Geochem. Geophy. Geosys., 7, Q12003, doi:10.1029/2006GC001323, 2006. 3608

Mashayek, A., Ferrari, R., Vettoretti, G., and Peltier, W. R.: The role of the geothermal heat flux in driving the abyssal ocean circulation, Geophys. Res. Lett., 40, 3144–3149, doi:10.1002/grl.50640, 2013. 3599

McDougall, T. J.: Neutral density surface in the ocean: implications for modelling, Geophys. Res. Lett., 14, 797–800, doi:10.1029/GL014i008p00797, 1987. 3609

Meehl, G. A., Stocker, T. F., Collins, W. D., Friedlingstein, P., Gaye, A. T., Gregory, J. M., Kitoh, A., Knutti, R., Murphy, J. M., Noda, A., Raper, S. C. B., Watterson, I. G., Weaver, A. J., and Zhao, Z.-C.: Global climate projections, in: Climate Change 2007: The Physical Science Basis. Contribution of Working Group I to the Fourth Assessment Report of the Intergovernmental Panel on Climate Change, edited by: Solomon, S., Qin, D., Manning, M., Chen, Z., Marquis, M., Averyt, K. B., Tignor, M., and Miller, H. L., Cambridge University Press, Cambridge, UK and New York, NY, USA, 2007. 3606

Monnin, E., Indermühle, A., Daellenbach, A., Flueckiger, J., Stauffer, B., Stocker, T. F., Raynaud, D., and Barnola, J.-M.: Atmospheric CO_2 concentrations over the Last Glacial Termination, Science, 291, 112–114, doi:10.1126/science.291.5501.112, 2001. 3600

Otto-Bliesner, B. L., Hewitt, C. D., Marchitto, T. M., Brady, E. C., Abe-Ouchi, A., Crucifix, M., Murakami, S., and Weber, S. L.: Last Glacial Maximum ocean thermohaline circulation: PMIP2 model intercomparisons and data constraints, Geophys. Res. Lett., 34, 1–6, doi:10.1029/2007GL029475, 2007. 3600

Petit, J. R., Jouzel, J., Raynaud, D., Barkov, N. I., Barnola, J.-M., Basile, I., Bender, M., Chappellaz, J., Davis, M., Delaygue, G., Delmotte, M., Kotlyakov, V. M., Legrand, M., Lipenkov, V. Y., Lorius, C., Pepin, L., Ritz, C., Saltzman, E., and Stievenard, M.: Climate and atmospheric history of the past 420,000 years from the Vostok ice core, Antarctica, Nature, 399, 429–436, 1999.

Ritz, S. P., Stocker, T. F., Grimalt, J. O., Menviel, L., and Timmermann, A.: Estimated strength of the Atlantic overturning circulation during the last deglaciation, Nat. Geosci., 6, 208–212, 2013. 3607

Impact of the oceanic geothermal heat flux on a glacial ocean state

M. Ballarotta et al.

Title Page

Abstract | Introduction

Conclusions | References

Tables | Figures

◀ | ▶

◀ | ▶

Back | Close

Full Screen / Esc

Printer-friendly Version

Interactive Discussion

Roquet, F., Madec, G., McDougall, T. J., and Barker, P. M.: Accurate polynomial expressions for the density and specific volume of seawater using the TEOS-10 standard, Ocean Model., 90, 29–43, 2015. 3601

Sarnthein, M., Winn, K., Jung, S. J. A., Duplessy, J. C., Labeyrie, L., Erlenkeuser, H., and Ganssen, G.: Changes in east Atlantic deep-water circulation over the last 30,000 years – 8 time slice reconstructions, Paleoceanography, 9, 209–267, 1994. 3600

Scott, J., Marotzke, J., and Adcroft, A.: Geothermal heating and its influence on the meridional overturning circulation, J. Geophys. Res., 106, 31141–31154, doi:10.1029/2000JC000532, 2001. 3599

Siegenthaler, U., Stocker, T. F., Monnin, E., Lüthi, D., Schwander, J., Stauffer, B., Raynaud, D., Barnola, J.-M., Fischer, H., Masson-Delmotte, V., and Jouzel, J.: Stable carbon cycle-climate relationship during the last Pleistocene, Science, 310, 1313–1317, doi:10.1126/science.1120130, 2005.

Skinner, L. C., Fallon, S., Waelbroeck, C., Michel, E., and Barker, S.: Ventilation of the deep Southern Ocean and deglacial CO_2 rise, Science, 328, 1147, doi:10.1126/science.1183627, 2010.

Stein, C. and Stein, S.: A model for the global variation in oceanic depth and heat flow with lithospheric age, Nature, 359, 123–129, doi:10.1038/359123a0, 1992. 3599

Tagliabue, A., Bopp, L., Roche, D. M., Bouttes, N., Dutay, J.-C., Alkama, R., Kageyama, M., Michel, E., and Paillard, D.: Quantifying the roles of ocean circulation and biogeochemistry in governing ocean carbon-13 and atmospheric carbon dioxide at the last glacial maximum, Clim. Past, 5, 695–706, doi:10.5194/cp-5-695-2009, 2009. 3608

Timmermann, R., Goosse, H., Madec, G., Fichefet, T., Ethe, C., and Dulière, V.: On the representation of high latitude processes in the ORCA-LIM global coupled sea ice-ocean model, Ocean Model., 8, 175–201, doi:10.1016/j.ocemod.2003.12.009, 2005. 3601

Toggweiler, J. R., Russell, J. L., and Carson, S. R.: Midlatitude westerlies, atmospheric CO_2, and climate change during the ice ages, Paleoceanography, 21, PA2005, doi:10.1029/2005PA001154, 2006.

Urakawa, L. and Hasumi, H.: A remote effect of geothermal heat on the global thermohaline circulation, J. Geophys. Res., 114, C07016, doi:10.1029/2008JC005192, 2009. 3599

Watson, A. J. and Garabato, A. C. N.: The role of Southern Ocean mixing and upwelling in glacial–interglacial atmospheric CO_2 change, Tellus B, 58, 73–87, doi:10.1111/j.1600-0889.2005.00167.x, 2006.

Impact of the oceanic geothermal heat flux on a glacial ocean state

M. Ballarotta et al.

Title Page

Abstract | Introduction

Conclusions | References

Tables | Figures

|◀ | ▶|

◀ | ▶

Back | Close

Full Screen / Esc

Printer-friendly Version

Interactive Discussion

Worthington, L.: Genesis and evolution of water masses, Meteor. Mon., 8, 63–67, 1968.

Zhang, X., Lohmann, G., Knorr, G., and Xu, X.: Different ocean states and transient characteristics in Last Glacial Maximum simulations and implications for deglaciation, Clim. Past, 9, 2319–2333, doi:10.5194/cp-9-2319-2013, 2013. 3601

5 Zhou, S., Qu, L., Zhao, X., and Wan, W.: Laboratory simulation of the influence of geothermal heating on the interior ocean, Acta Oceanol. Sin., 33, 25–31, doi:10.1007/s13131-014-0512-8, 2014. 3599

Impact of the oceanic geothermal heat flux on a glacial ocean state

M. Ballarotta et al.

Title Page

Abstract | Introduction

Conclusions | References

Tables | Figures

|◄ | ►|

◄ | ►

Back | Close

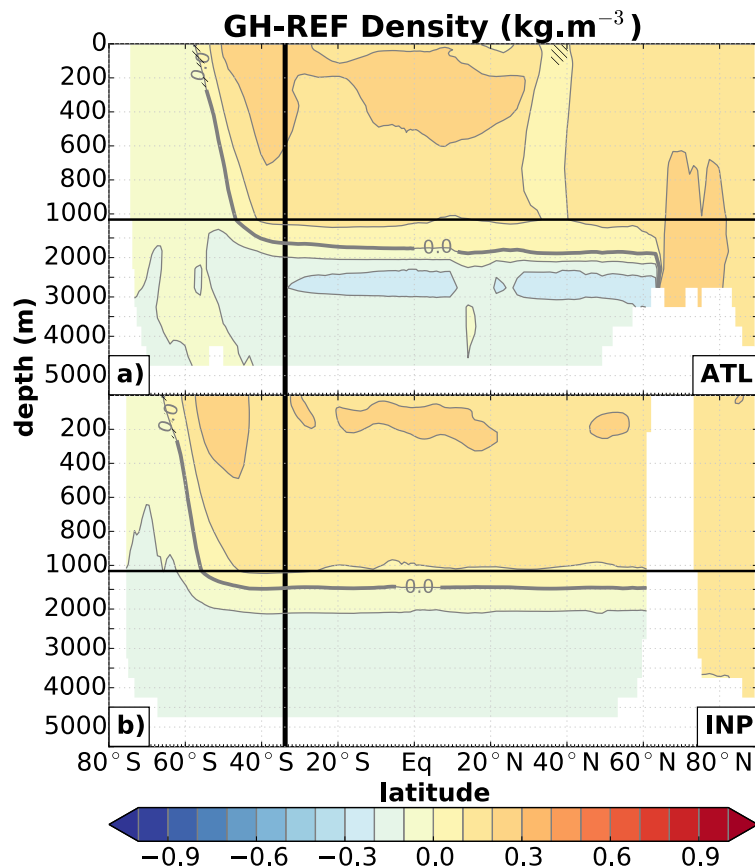Full Screen / Esc

Printer-friendly Version

Interactive Discussion
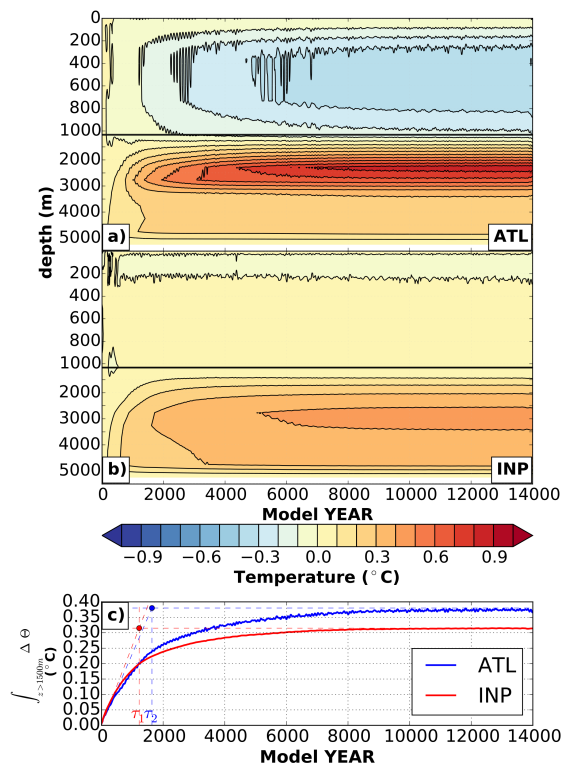
Figure 1. Annual mean potential temperature drift (in °C) induced by the geothermal heat forcing as a function of depth averaged in **(a)** the Atlantic basin and **(b)** the Indo-Pacific basin. Contour intervals are every 0.1 °C. Note the vertical scale is increased in the upper 1000 m. **(c)** Time-series of the mean temperature accumulation (in °C) due to the geothermal heat below 1500 m in the Atlantic and Indo-Pacific basins. $\tau_1 \sim 1200$ years and $\tau_2 \sim 1600$ years denote the characteristic time scale, i.e. the amount of time required for the response to reach $(1 - 1/e) \approx 63\%$ of the maximum heat accumulation, in the Indo-Pacific and the Atlantic basins.
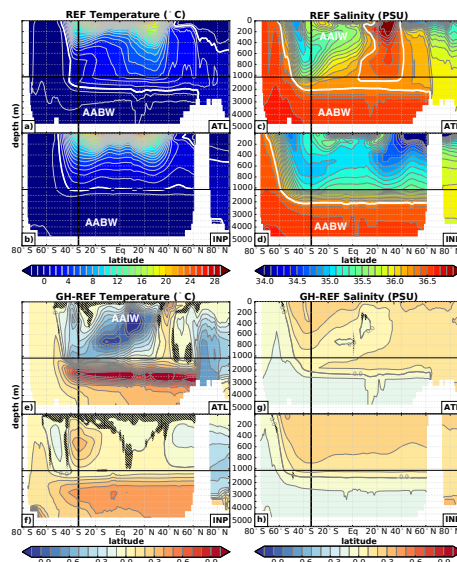
Figure 2. Annual zonal mean potential temperature patterns (in ˚C) in the reference experiment (REF) for **(a)** the Atlantic basin, **(b)** the Indo-Pacific basin (Contour interval every 1 ˚C, thick white contour is 0 ˚C); salinity patterns (in ˚C) in the reference experiment (REF) for **(c)** the Atlantic basin, **(d)** the Indo-Pacific basin (Contour interval every 0.1 PSU, thick white contour is 36.3 PSU); the temperature difference between REF and GH for **(e)** the Atlantic basin, and **(f)** the Indo-Pacific basin (Contour interval every 0.1 ˚C, thick grey contour is 0 ˚C); and salinity difference between REF and GH for **(g)** the Atlantic basin, and **(h)** the Indo-Pacific basin (Contour interval every 0.1 PSU, thick white contour is 0 PSU). The thick vertical black line shows the location of the South Atlantic entrance at 34˚ S. Note the vertical scale is increased in the upper 1000 m. The patterns in each Southern Ocean sector are shown in each panel between 80 and 34˚ S. The dashed contours represent the region where the difference is insignificant at a 95 % confidence level (based on a *t* test). AABW: Antarctic Bottom Water, AAIW: Antarctic Intermediate Water.

Figure 3. Map of the annual mean temperature difference (in ˚C) between GH and REF at 2500 m. Maximum and minimum values are denoted in the lower left corner. The largest warming is in the Atlantic deep western boundary current.
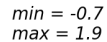
Figure 4. Difference in the annual mean and zonal mean potential density patterns (σ_4 in kg m^{-3}) between REF and GH for **(a)** the Atlantic basin, and **(b)** the Indo-Pacific basin. Contour and scale same as in Fig. 2
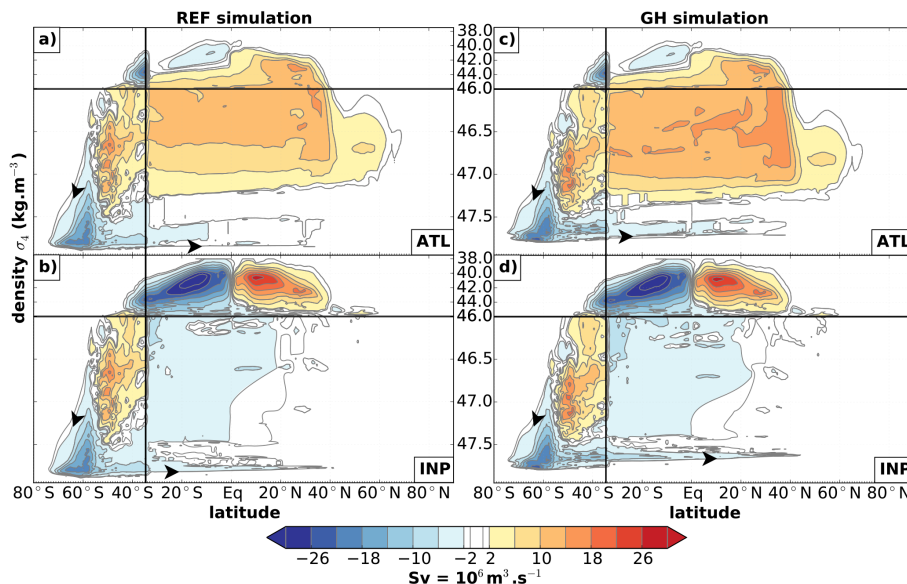
Figure 5. Annual mean density-binned effective (Eulerian + eddy-induced velocities) meridional overturning circulation (in Sv) in the experiment *without* geothermal heating (REF) for **(a)** the Atlantic basin, and **(b)** the Indo-Pacific basin; and in the experiment *with* geothermal heating (GH) for **(c)** the Atlantic basin, and **(d)** the Indo-Pacific basin. The thick black line shows the location of the South Atlantic entrance at 34° S. The annual mean meridional overturning circulation in the Southern Ocean is shown in each panel between 80 and 34° S. Positive (negative) contours represent clockwise (anti-clockwise) circulations. Contour interval is every 4 Sv, and −1 and +1 Sv contours are added. Density bins intervals every 0.01 kg m^{-3}. Note the vertical scale is increased for $\sigma_4 > 46$ kg m^{-3}.

Full Screen / Esc

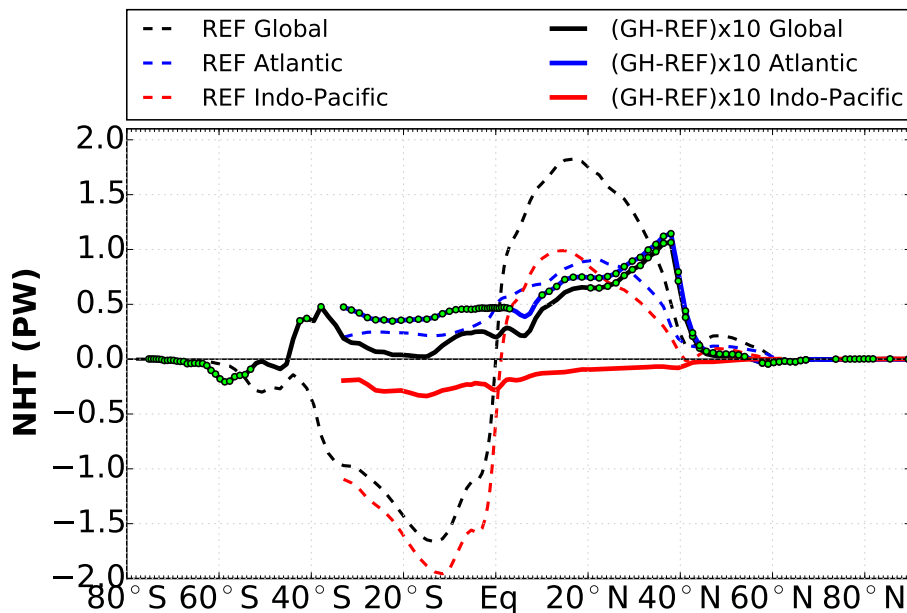Printer-friendly Version

Interactive Discussion
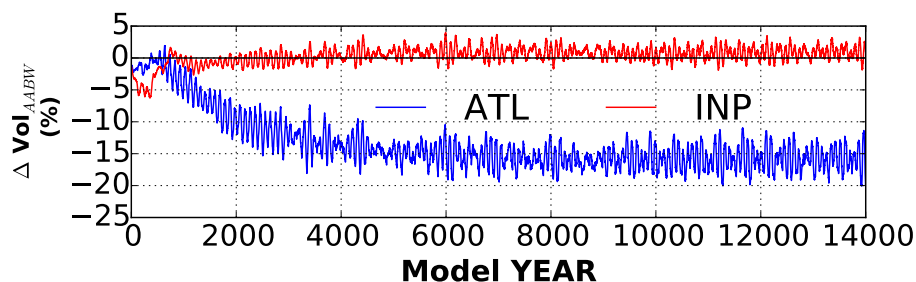
Figure 6. Time-series of the AABW volume variation (in %) in the Atlantic and Indo-Pacific basins. The AABW volume is computed as the volume of water below 2000 m where the annual mean effective overturning circulation in latitude-depth coordinates is negative (Fig. 8a, b).

Figure 7. Annual mean effective (Eulerian mean + eddy-induced velocities) northward heat transport (in PW = 10^{15} W) in the Global Ocean, the Atlantic and the Indo-Pacific basins in the reference experiment (dashed line); and the difference between REF and GH in the annual mean northward heat transport (thick line). Note that the difference is magnified by a factor 10. The green dots show where the difference is significant at a 95 % confidence level (based on a t test).

Discussion Paper | Discussion Paper | Discussion Paper | Discussion Paper |

CPD

11, 3597–3624, 2015

Impact of the oceanic geothermal heat flux on a glacial ocean state

M. Ballarotta et al.

Title Page

Abstract | Introduction

Conclusions | References

Tables | Figures

|◀ | ▶|

◀ | ▶

Back | Close

Full Screen / Esc

Printer-friendly Version

Interactive Discussion
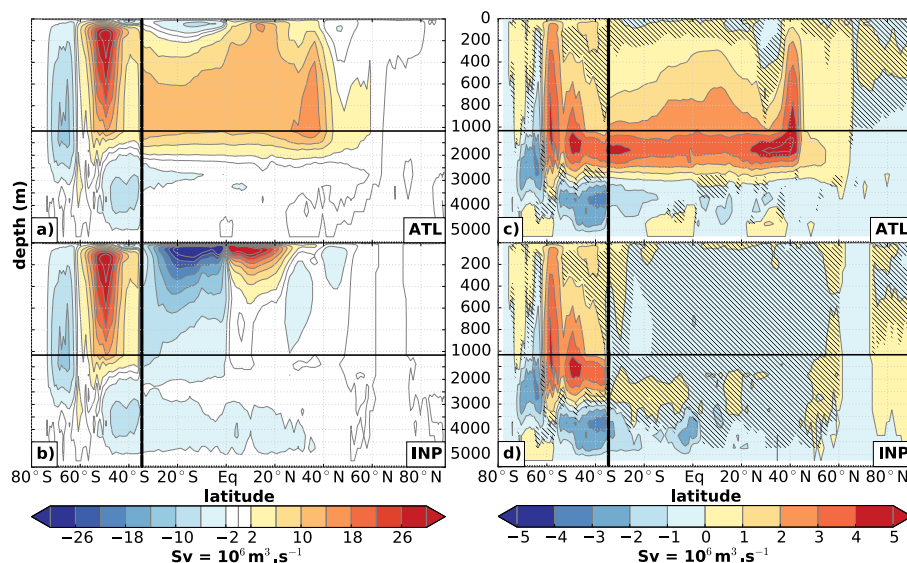
Figure 8. Annual mean effective (Eulerian mean + eddy-induced velocities) meridional over-turning circulation in latitude-depth coordinates (in $Sv = 10^6\,m^3\,s^{-1}$) in the reference experi-ment (REF) for **(a)** the Atlantic basin, and **(b)** the Indo-Pacific basin. Contour interval is every 4 Sv, and the 0 Sv contours is added. Positive (negative) values represent clockwise (counter-clockwise) circulation. Difference in the effective meridional overturning circulation between REF and GH for **(c)** the Atlantic basin, and **(d)** the Indo-Pacific basin. Contour interval is every 1 Sv. The annual mean meridional overturning circulation and the difference in the meridional overturning circulation in the Southern Ocean between GH and REF is shown 80 and 34° S. Note the vertical scale is increased in the upper 1000 m. The dashed contours represent the region where the difference is insignificant at a 95 % confidence level (based on a t test).